


New Challenges on Developing Experimental Methods for Innovative Metal Forming Techniques [†]

Ruiqiang Zhang and Jianguo Lin * 

Department of Mechanical Engineering, Imperial College London, London SW7 2BX, UK

* Correspondence: jianguo.lin@imperial.ac.uk

[†] Presented at 19th International Conference on Experimental Mechanics, Kraków, Poland, 17–21 July 2022.

Abstract: For industrial applications of innovative metal forming techniques, advanced experimental methods have been developed to characterize the mechanical properties of materials under the corresponding forming conditions. This paper focuses on uniaxial tensile tests for the characterization of the thermomechanical behavior of materials and biaxial tensile tests for the evaluation of the material formability under hot-stamping conditions; these test methods have been improved in recent years. Applications of both the uniaxial and biaxial tensile tests to a boron steel sheet are presented, and the associated experimental results are analyzed. Importantly, new challenges encountered in the development of these experimental methods are discussed and summarized. This paper concludes that more efforts are needed for the standardization of these experimental methods in future.

Keywords: hot-stamping; uniaxial tensile test; biaxial tensile test; cruciform specimen; thermomechanical behavior; formability; forming limit curves



Citation: Zhang, R.; Lin, J. New Challenges on Developing Experimental Methods for Innovative Metal Forming Techniques. *Phys. Sci. Forum* **2022**, *4*, 15. <https://doi.org/10.3390/psf2022004015>

Academic Editors: Zbigniew L. Kowalewski and Elżbieta Pieczyskasz

Published: 5 August 2022

Publisher's Note: MDPI stays neutral with regard to jurisdictional claims in published maps and institutional affiliations.



Copyright: © 2022 by the authors. Licensee MDPI, Basel, Switzerland. This article is an open access article distributed under the terms and conditions of the Creative Commons Attribution (CC BY) license (<https://creativecommons.org/licenses/by/4.0/>).

1. Introduction

To improve energy efficiency and reduce CO₂ emissions [1], hot-stamping techniques have been developed in recent years for ultra-high strength steels [2] and high-strength aluminum alloys [3] and applied to manufacture light panel components with complex geometries for vehicle body structures such as door rings, bumpers, roof rails, and chassis [4]. According to a recent study, over 600 million hot-stamped parts of boron steels were produced annually for passenger cars alone, and 10% by mass of a typical body in white (BiW) was made with using hot-stamping on average, with some vehicles pushing 40% (e.g., 2014 Volvo XC90 [4]). Figure 1a shows a hot-stamping process for steels schematically [5], which includes heating the materials above the austenite formation temperature (e.g., about 925 °C) in a furnace, transferring them from the furnace into forming tools quickly, forming and quenching the materials simultaneously into components with target shapes, and then transferring the formed components out of the forming tools. During the hot-stamping of steels, the formability of the materials with a full austenite microstructure can be improved significantly, which makes it possible to form components with complex geometries. Furthermore, the steel components after hot-stamping could have an ultimate tensile strength (UTS) up to 1700 MPa thanks to the formation of a full martensite microstructure [6].

For industrial applications of the hot-stamping techniques, it is essential to characterize the thermomechanical behavior of materials under hot-stamping conditions. Figure 1b shows a commonly used thermal cycle, which mimics the industrial hot-stamping process, for boron steel 22MnB5, for thermomechanical tests [7]. In the thermal cycle, the material is heated to the austenite temperature of 925 °C and after soaking it for 60 s at this temperature, it is quenched at a cooling rate of 60 °C/s to a target temperature (e.g., 800 °C), followed by deformation at the target temperature and strain rate. Different from the tests under cold or warm forming conditions, the thermomechanical tests under hot-stamping conditions are extremely challenging due to the difficulty of accurately replicating the

thermal cycle illustrated in Figure 1b. To overcome this difficulty, the Gleeble material simulator (Poestenkill, NY, USA) has been widely used for tests under hot-stamping conditions [8,9] because it is capable of either heating specimens using resistance heating or cooling them using a quenching system at a high cooling rate, along with thermocouples providing signals for the accurate feedback control of specimen temperature within ± 1 °C.

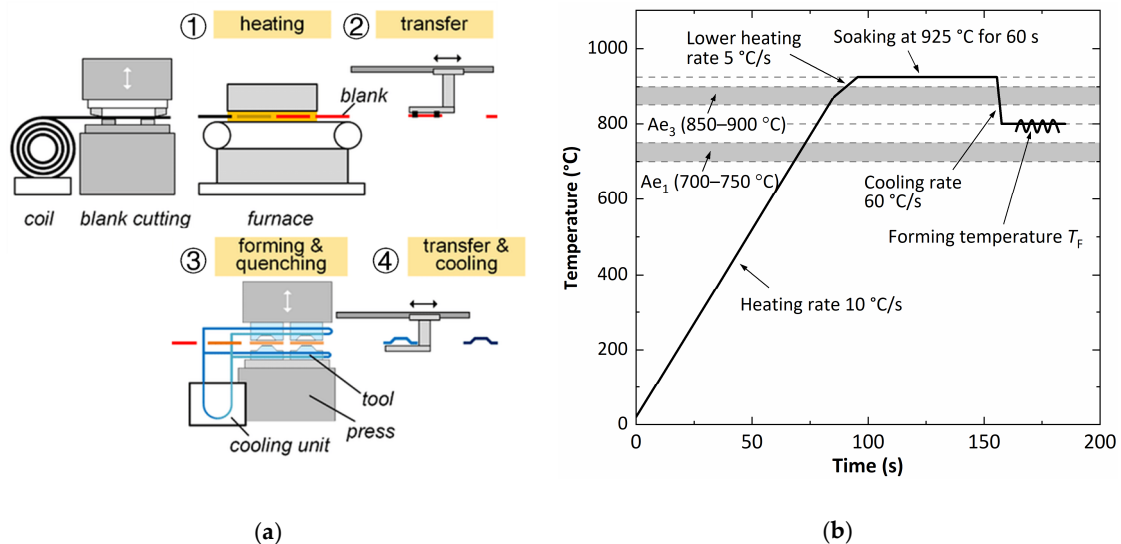


Figure 1. Schematic diagrams showing industrial hot-stamping: (a) a hot-stamping process including heating, transfer, forming and quenching, and transfer and cooling; (b) a thermal cycle to mimic the industrial hot-stamping conditions for boron steel 22MnB5 [7].

In this paper, recent thermomechanical experimental methods for hot-stamping applications are presented. These experimental methods include the uniaxial tensile tests for the characterization of thermomechanical behavior and the biaxial tensile tests for the determination of the formability data; these tests have been used and improved in recent years. The uniaxial tensile tests use dog-bone specimens, while the biaxial tensile tests employ cruciform specimens. Applications of these experimental method to a boron steel sheet are recalled, and the associated experimental data are analyzed and discussed. Based on the review mentioned above, existing challenges are summarized for the further development of these experimental methods.

2. Uniaxial Tensile Tests for Thermomechanical Behavior Characterization

2.1. Methods of Specimen Heating and Temperature Control

Following the thermal cycle (Figure 1b) to mimic the hot-stamping conditions, Zhang et al. [10] conducted uniaxial tensile tests on a 1.5 mm thick boron steel 22MnB5 sheet using the Gleeble 3800 to characterize the thermomechanical behavior of the material. Figure 2a shows the heating scheme of the dog-bone specimens using resistance heating in Gleeble, in which both ends of each specimen were connected to positive and negative electrodes respectively, and a pair of thermocouples was welded at the specimen center for the feedback control of the specimen temperature. The other two pairs of thermocouples were welded at the locations with a distance from the specimen center of 10 and 20 mm respectively, for the measurement of the temperature distributions along the specimen length direction. Figure 2b presents the results of the temperature distributions when the temperature at the specimen center reached different target values steadily. It was found that the temperature distribution was nonuniform, and the temperature decreased with increasing distance from the specimen center. For example, a decrease of 6.5 °C was observed at the location of 10 mm when the temperature at the center reached 750 °C, while it became 43 °C at the location of 20 mm. The temperature decrease was caused due to the heat loss to the specimen ends and the attached jaw carriers in the Gleeble, in which the

carriers are cooled using water for protection against heating. A similar phenomenon was also observed in the other tests under hot-stamping conditions [11,12]. Considering the resistance heating method and the protection of the Gleeble carriers, this nonuniformity of the temperature distribution in the dog-bone specimens is inevitable.

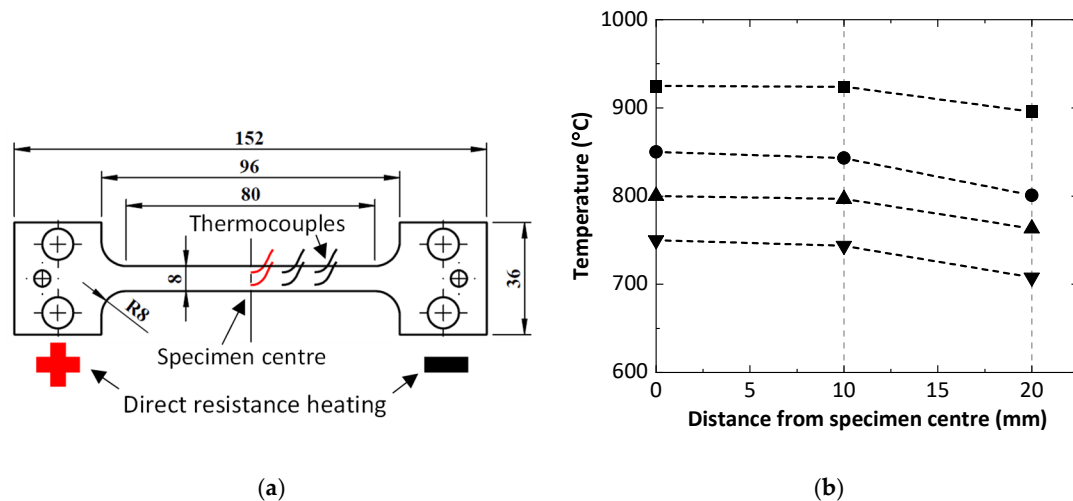


Figure 2. Resistance heating of dog-bone specimens for uniaxial tensile tests at high temperatures [10]: (a) setup of resistance heating together with the thermocouples welded at the specimen center providing signals for feedback control of the specimen temperature and (b) temperature distributions along the specimen length direction.

2.2. Control of Strain Rates

The nonuniform temperature distribution (Figure 2b) in the dog-bone specimens results in several challenges in the uniaxial tensile tests under hot-stamping conditions. One of the challenges is the control of strain rates to reach target values during the whole deformation. In order to analyze both the distribution and evolution of strain rates, Zhang et al. [10] successfully applied the digital image correlation (DIC) to the measurement of a full strain field in the tests on boron steels under hot-stamping conditions. In order to achieve constant strain rates, displacements to stretch the specimens were controlled using the equation $\Delta l = l_0 \cdot [\exp(t \cdot \dot{\epsilon}_T) - 1]$, where Δl is the increment of the displacement, l_0 is the gauge length, t is the time, $\dot{\epsilon}_T$ is the target strain rate. Figure 3a shows the strain fields at different normalized times, t/t_F , measured using the DIC of the boron steel specimen at 750 °C and 0.2 /s. It was found that the strains along the specimen length direction were nonuniformly distributed even at the early stages of deformation (e.g., $t/t_F = 0.2$ or 0.5). This was caused by the nonuniform temperature distributions, and more deformation occurred near the specimen center where the temperatures were higher.

Figure 3b shows the average strain rates within several different gauge lengths (i.e., 2, 6, 12, 26 and 40 mm). As can be seen, the strain rates were significantly dependent on the gauge length, especially at the later stages of deformation. The reason of this dependency is the localized deformation near the specimen center partly due to the nonuniform temperature. Someone may argue that this was caused by the occurrence of diffuse necking, but the divergence of the strain rates among the different gauge lengths occurred very early. Furthermore, the strain rates were not constant but increased with increasing deformation time, especially for a smaller gauge length. For example, the strain rates within the gauge length of 2 mm were about 0.1 /s at the initial stages of deformation, and they increased to about 1.8 /s at fracture, which was 800% higher than the target value of 0.2 /s. This means that due to the nonuniform temperature distributions, the constant strain rates cannot be achieved using the commonly used method of controlling the displacement to stretch specimens, and a new method is needed in the future.

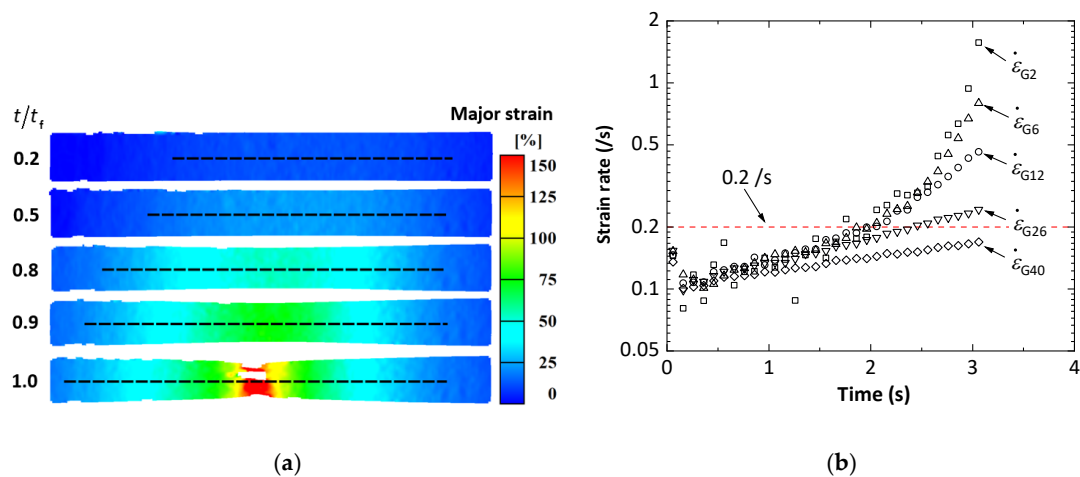


Figure 3. Strain fields and strain rates of the boron steel specimen deformed at 750 °C and 0.2 /s [10]: (a) strain fields in the parallel reduced region at different normalized times and (b) the evolution of strain rates based on different gauge lengths during deformation.

2.3. Dependency of Stress–Strain Curves on Gauge Lengths

The other challenge caused by the nonuniform temperature distributions is the high dependency of stress–strain curves on gauge lengths. Zhang et al. [10] obtained the engineering stress–strain curves of the boron steel under hot-stamping conditions by using the average strains within the different gauge lengths from 2 to 40 mm. Figure 4 presents the results at 750 and 850 °C, respectively. As can be seen in Figure 4, the stress–strain curves were significantly dependent on the gauge lengths; a divergency of the stress–strain curves among the different gauge lengths appeared even though the engineering strain was relatively small. This is partly because the deformation along the specimen length direction was localized even at the early stages of the deformation due to the nonuniform temperature distributions. The high dependency of stress–strain curves on gauge lengths means the uncertainties of the characterized mechanical behavior (e.g., ductility) of the material. It is worth noting that, for tests at room temperature, a long gauge length, which is at least 5 times the specimen width, is usually recommended. However, this rule is not applicable to the tests at high temperatures investigated in this study because, with a long gauge length, there exists a considerable difference between the strain rates at the end of the gauge length and at the specimen center. Therefore, a standard of selecting a gauge length for the characterization of stress–strain curves in tests at high temperatures is needed.

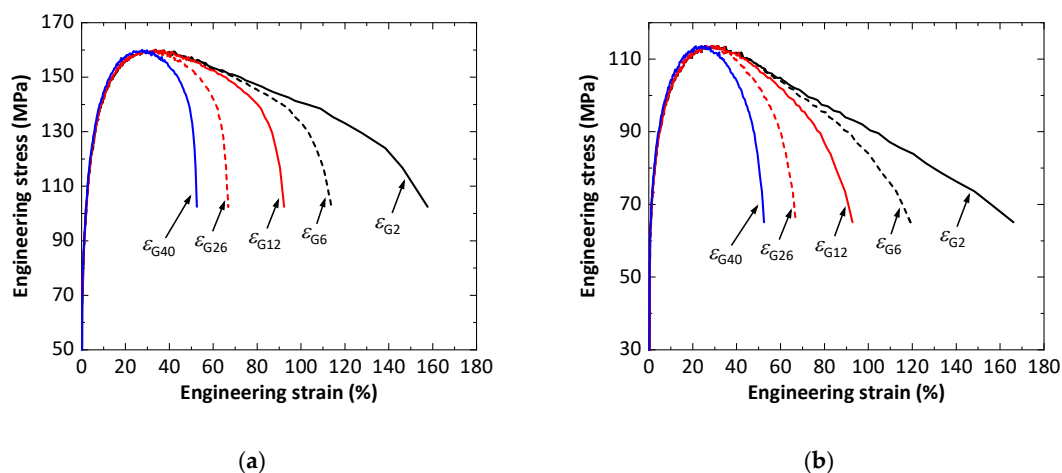


Figure 4. Engineering stress–strain curves of boron steel based on different gauge lengths under different test conditions [10]: (a) 750 °C and 0.2 /s and (b) 850 °C and 0.2 /s.

3. Biaxial Tensile Tests for Formability Evaluation

3.1. A Recent Novel Biaxial Test Method

To evaluate the formability of materials under hot-stamping conditions, such as boron steels, Zhang et al. [7] developed a novel biaxial test method that comprises a biaxial tensile system, cruciform specimens, and a spatio-temporal method. In this method, as shown in Figure 5, the biaxial tensile system is used to heat the cruciform specimens using a direct resistance heating system to replicate the hot-stamping thermal cycles and then to deform the specimens in different strain states, along with a DIC system for the measurement of the strain fields in the gauge area. Based on the measured strain fields, the spatio-temporal method, which was first introduced by Zhang et al. [13,14], is used to determine the necking and fracture limit strains and then to construct forming limit curves (FLCs) and fracture forming limit curves (FFLCs), which are common tools for formability evaluation.

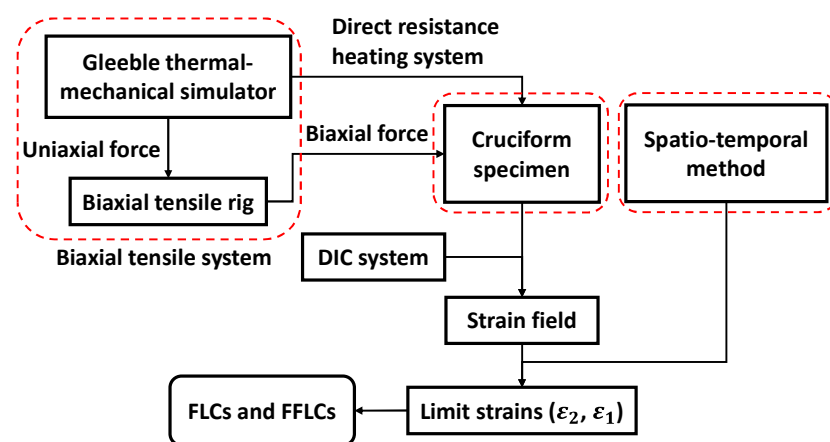


Figure 5. A recent novel biaxial test method for formability evaluation under hot-stamping conditions, comprising a biaxial tensile system to stretch cruciform specimens in different strain states until fracture, along with the measurement of strain fields using the DIC, and a spatio-temporal method to determine the necking and fracture limit strains [7].

3.2. Specimen Design, Heating Method, and Temperature Control

In biaxial tensile tests for the formability evaluation, it is critical to initiate localized necking near the center of the cruciform specimens for producing linear strain paths [15]. For this purpose, Zhang et al. [7] designed a new cruciform specimen as shown in Figure 6a and proposed an associated heating scheme, in which the upper end of the specimen is connected to a positive electrode, and the lower end is connected to a negative electrode. In the central region of each specimen, there is a gauge area, which is thinned to have a dome profile through the thickness direction so as to localize most of the deformation in this area. Figure 6b shows the temperature evolutions at the specimen center and at locations A and C (marked in Figure 6a), together with an insert image showing the temperature distribution in the central region of the boron steel 22MnB5 specimen when the temperature at the specimen center reached a steady 925 °C. As can be seen, the temperature at the specimen center was higher than at A and C, which indicated that the temperature distribution in the gauge area was nonuniform. This nonuniformity was further validated using the results from thermal finite element (FE) simulations under the same conditions [7], as shown in Figure 6c. According to the FE results, the temperature distributions were symmetrical to the arm directions and were nonuniform in the gauge area. It should be noted that the gauge area has a higher temperature and smaller thickness compared to the other regions, which makes it possible to initiate the localized necking in this area.

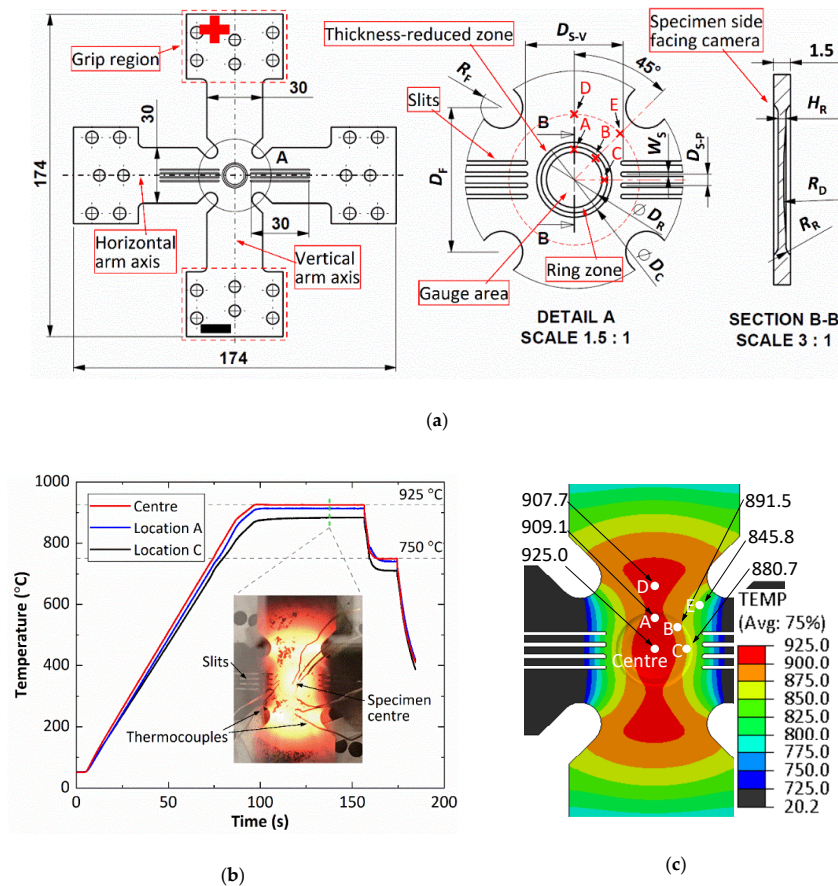


Figure 6. Cruciform specimen design and heating for formability evaluation under hot-stamping conditions [7]: (a) cruciform specimen design together with the heating scheme using the direct resistance heating method, (b) temperature evolution at the preselected locations with the inset showing the temperature distribution in the gauge area of a boron steel specimen, and (c) temperature distribution simulated using thermal FE model under the same conditions.

3.3. Strain Distribution in Gauge Area and Strain Path

Similarly to the uniaxial tests mentioned above, the nonuniformity of the temperature distributions in the gauge area of the cruciform specimens results in nonuniform strain distributions in this area [7]. Figure 7a shows the thickness reduction in the gauge area of the specimen in an equi-biaxial tension at different normalized times (i.e., $t/t_F = 0.9$ and 1). As can be seen, the thickness reduction was nonuniform but concentrated near the specimen center because of the higher temperature and smaller thickness. The strain fields were analyzed using the spatio-temporal method to determine the necking and fracture limit strains. In this method, a base zone (BZ) and a reference zone (RZ) were selected around the fracture initiation location, and then the average strains within the BZ were used as the strain path, along with the limit strains determined with the help of the average strains within the RZ. Figure 7b presents the results, including strain path and limit strains, for the specimen deformed in the equi-biaxial tension. It can be seen in this figure that the strain path was almost linear, but the associated strain ratio β (the ratio of the increments of minor strain to major strain) was 0.45, which was lower than the theoretical value of 1 for an isotropic material. The low strain ratio in the above test may be caused by the different designs between the horizontal and vertical arms, nonuniform temperature distributions, etc. Therefore, either the specimen design or the temperature distribution needs to be improved to obtain strain ratios that are close to 1 in equi-biaxial tensions.

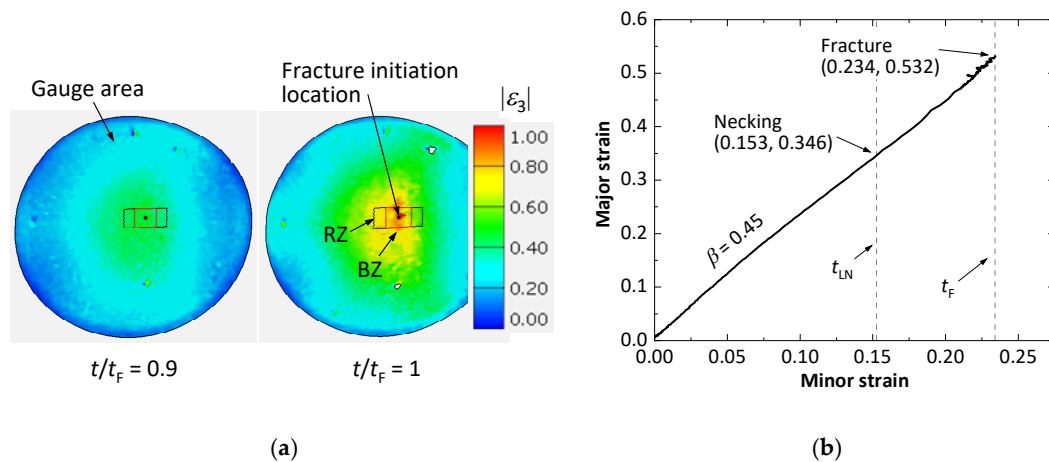


Figure 7. Cruciform specimen of boron steel deformed in biaxial tension at 800 °C and 0.1 /s [7]: (a) strain distributions in the gauge area at different normalized times; (b) strain path in the BZ, along with the necking and fracture limit strains (BZ: base zone, RZ: reference zone).

3.4. Recent Results on The Formability Data of Boron Steel

Using an innovative biaxial test method, Zhang et al. [7] constructed both FLCs and FFLCs for the boron steel sheet by carrying out the biaxial tests in different strain states under hot-stamping conditions. Figure 8a presents the damaged specimens at 800 °C and 0.1/s in equi-biaxial, plane-strain, and uniaxial tensions. As can be seen, all fractures indeed occurred close to the specimen center of the gauge area. After analyzing the strain fields and obtaining the associated limit strains, both the FLCs and FFLCs for the boron steel were determined, and Figure 8b shows the results at a strain rate of 0.1 /s and the different temperatures. Furthermore, the formability of the material was highly dependent on the strain states, and it became the lowest when the strain states were between plane-strain and equi-biaxial but were closer to the former. In addition, the formability of the material increased with increasing temperature, but it changed little in the range of the temperature investigated in the present study. These experimental data of FLCs and FFLCs provide possibilities for the formulation and calibration of the viscoplastic constitutive models for formability evaluation for industrial hot-stamping applications.

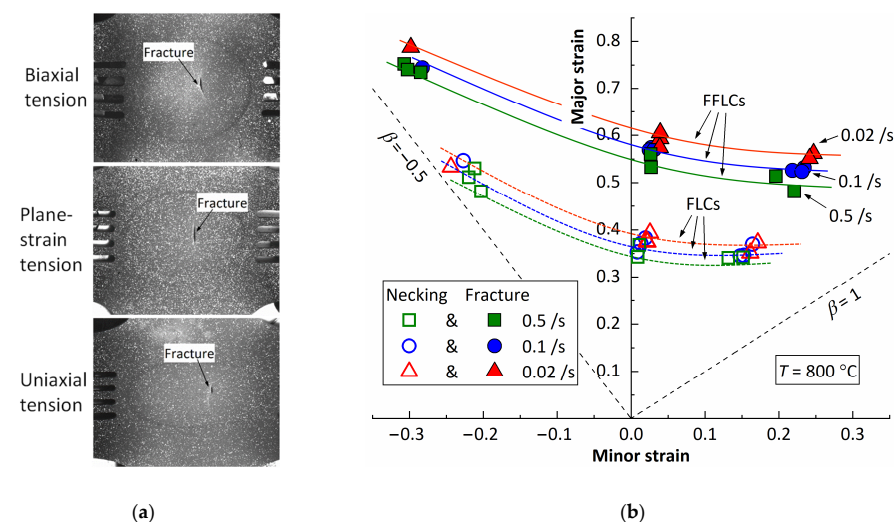


Figure 8. FLCs and FFLCs for boron steel determined using the novel biaxial test method [7]: (a) damaged cruciform specimens at 800 °C and 0.1 /s in different strain states and (b) FLCs and FFLCs determined for boron steel at a strain rate of 0.1 /s and different temperatures.

4. Conclusions

Advanced experimental methods have been applied to characterize the thermomechanical behavior of materials for the applications of innovative metal forming techniques. In uniaxial tensile tests in which specimens are heated using the resistance heating, the temperature at the specimen center was the highest, and it decreased with increasing distance from the specimen center. The nonuniform temperature distribution resulted in nonuniform deformation along the gauge length and further led to nonuniform strain rates and uncertainties about the mechanical properties characterized using the tests. The biaxial test method has been developed and successfully applied to boron steel sheets for the determination of FLCs and FFLCs under hot-stamping conditions for the first time. However, the gauge area of the cruciform specimen experienced nonuniform temperature distributions, which partly resulted in the nonuniform deformation in this area. In addition, it was difficult to produce an equi-biaxial strain state in the gauge area because the temperature distributions are nonuniform, and the horizontal arms of each cruciform specimen were different from the vertical arms.

Author Contributions: Conceptualization, R.Z. and J.L.; methodology, R.Z. and J.L.; software, R.Z.; validation, R.Z.; formal analysis, R.Z.; investigation, R.Z.; resources, J.L.; data curation, R.Z.; writing—original draft preparation, R.Z.; writing—review and editing, J.L.; visualization, J.L.; supervision, J.L.; project administration, J.L.; funding acquisition, J.L. All authors have read and agreed to the published version of the manuscript.

Funding: This research was funded by the Engineering and Physical Sciences Research Council (EPSRC), grant number EP/R001715/1.

Conflicts of Interest: The authors declare no conflict of interest. The funders had no role in the design of the study; in the collection, analyses, or interpretation of data; in the writing of the manuscript, or in the decision to publish the results.

References

1. Zacharof, N.G.; Fontaras, G.; Ciuffo, B.; Tsiakmakis, S.; Anagnostopoulos, K.; Marotta, A.; Pavlovic, J. *Review of in Use Factors Affecting the Fuel Consumption and CO₂ Emissions of Passenger Cars*; European Commission: Brussels, Belgium, 2016. [\[CrossRef\]](#)
2. Manufacturing a Hardened Steel Article. GB 1490535 A, 11 December 1977.
3. Lin, J.; Dean, T.A.; Garrett, R.P.; Foster, A.D. Process for Forming Metal Alloy Sheet Components. WO 2008059242 A2, 22 May 2008.
4. Taylor, T.; Clough, A. Critical review of automotive hot-stamped sheet steel from an industrial perspective. *Mater. Sci. and Technol.* **2018**, *34*, 809–861. [\[CrossRef\]](#)
5. Karbasian, H.; Tekkaya, A.E. A review on hot-stamping. *J. Mater. Process. Technol.* **2010**, *210*, 2103–2118. [\[CrossRef\]](#)
6. Tong, C.; Rong, Q.; Yardley, V.A.; Li, X.; Luo, J.; Zhu, G.; Shi, Z. New Developments and Future Trends in Low-Temperature Hot-stamping Technologies: A Review. *Metals* **2020**, *10*, 1652. [\[CrossRef\]](#)
7. Zhang, R.; Shi, Z.; Yardley, V.A.; Lin, J. Experimental studies of necking and fracture limits of boron steel sheet under hot-stamping conditions. *J. Mater. Process. Technol.* **2022**, *302*, 117481. [\[CrossRef\]](#)
8. Merklein, M.; Lechler, J. Investigation of the thermo-mechanical properties of hot-stamping steels. *J. Mater. Process. Technol.* **2006**, *177*, 452–455. [\[CrossRef\]](#)
9. Li, N.; Lin, J.; Balint, D.S.; Dean, T.A. Experimental characterisation of the effects of thermal conditions on austenite formation for hot-stamping of boron steel. *J. Mater. Process. Technol.* **2016**, *231*, 254–264. [\[CrossRef\]](#)
10. Zhang, R.; Shao, Z.; Lin, J.; Dean, T.A. Measurement and analysis of heterogeneous strain fields in uniaxial tensile tests for boron steel under hot-stamping conditions. *Exp. Mech.* **2020**, *60*, 1289–1300. [\[CrossRef\]](#)
11. Shao, Z.; Li, N.; Lin, J.; Dean, T.A. Strain measurement and error analysis in thermo-mechanical tensile tests of sheet metals for hot-stamping applications. *Proc. Inst. Mech. Eng. Part C J. Mech. Eng. Sci.* **2018**, *232*, 1994–2008. [\[CrossRef\]](#)
12. Ganapathy, M.; Li, N.; Lin, J.; Abspoel, M.; Bhattacharjee, D. A novel grip design for high-accuracy thermo-mechanical tensile testing of boron steel under hot-stamping conditions. *Exp. Mech.* **2018**, *58*, 243–258. [\[CrossRef\]](#)
13. Zhang, R.; Shi, Z.; Shao, Z.; Dean, T.A.; Lin, J. A novel spatio-temporal method for determining necking and fracture strains of sheet metals. *Int. J. Mech. Sci.* **2021**, *189*, 105977. [\[CrossRef\]](#)
14. Zhang, R.; Shi, Z.; Shao, Z.; Yardley, V.A.; Lin, J. An effective method for determining necking and fracture strains of sheet metals. *MethodsX* **2021**, *8*, 101234. [\[CrossRef\]](#) [\[PubMed\]](#)
15. Zhang, R.; Shao, Z.; Shi, Z.; Dean, T.A.; Lin, J. Effect of cruciform specimen design on strain paths and fracture location in equi-biaxial tension. *J. Mater. Process. Technol.* **2021**, *289*, 116932. [\[CrossRef\]](#)